

## Coupled phonon–plasmon modes in indium phosphide observed by an ultrafast pump–probe technique

This article has been downloaded from IOPscience. Please scroll down to see the full text article.

2005 J. Phys.: Condens. Matter 17 5577

(<http://iopscience.iop.org/0953-8984/17/36/013>)

View [the table of contents for this issue](#), or go to the [journal homepage](#) for more

Download details:

IP Address: 129.252.86.83

The article was downloaded on 28/05/2010 at 05:54

Please note that [terms and conditions apply](#).

# Coupled phonon–plasmon modes in indium phosphide observed by an ultrafast pump–probe technique

O V Misochko and T N Fursova

Institute of Solid State Physics, Russian Academy of Sciences, 142432 Chernogolovka, Moscow region, Russia

Received 10 May 2005, in final form 28 July 2005

Published 26 August 2005

Online at [stacks.iop.org/JPhysCM/17/5577](http://stacks.iop.org/JPhysCM/17/5577)

## Abstract

We demonstrate that coupled phonon–plasmon modes in indium phosphide can be studied by a time-domain technique by reporting the results of the ultrafast study of differently doped electron- and hole-type InP semiconductors. We have observed coherent oscillations whose spectra comprise both phonon and plasmon modes. In p-type samples, the ultrafast pulses drive lattice modes that are coupled to the collective hole excitations for short time delays only. In contrast, electron plasma seems to be coupled more strongly to the lattice and, as a result, the decay time of the coherence for the plasma modes is extended.

Experiments carried out over the last decade have shown that ultrafast laser pulses can coherently excite collective modes of lattice (phonons) and electrons (plasmons) in semiconductors [1, 2]. Systems prepared with ultrashort pulses in a coherent state can provide additional, complementary information on the lattice and carrier dynamics as compared to conventional frequency-domain studies [3, 4].

The A<sup>III</sup>B<sup>V</sup> semiconductors, such as GaAs and InP, are technologically important materials with promising applications. Knowledge of the electronic and phononic properties that determine the fast response is a prerequisite for many applications. The phonon and electron properties of GaAs have been thoroughly studied in both time and frequency domains, and the existence of coupled phonon–plasmon modes in the time domain has been reported [5, 6]. While the amount of information obtained in the frequency domain for InP is comparable to that for GaAs, time-domain studies of this compound have been sporadic, and only a few of them have been carried out with femtosecond resolution [7–9]. Herein we report our results obtained with a femtosecond pump–probe technique on the lattice and carrier dynamics in n- and p-doped InP.

Our optical measurements were performed on (001)-oriented epitaxial films of InP with two different carrier concentrations for each kind of doping,  $10^{18}$  and  $4 \times 10^{18} \text{ cm}^{-3}$ . The zincblende structure of the material allows optical excitation of transverse and longitudinal optical phonons (TO and LO) and, in addition, the photoexcited plasma can sustain plasmons. Due to the polar character of the structure, the LO phonon interacts with the macroscopic electric

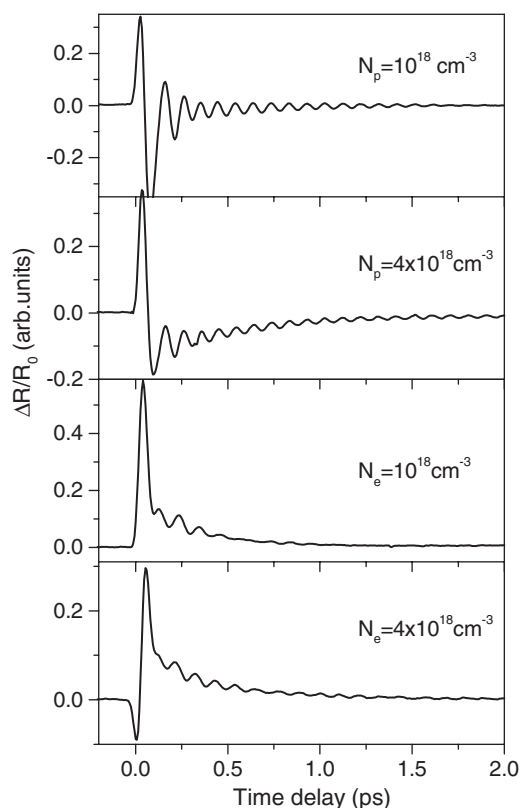


**Figure 1.** Differential reflectivity as a function of time delay for differently doped InP films with the free carrier concentrations shown in each panel.

field of the plasmon, giving rise to LO–plasmon coupled modes (LOPCM). The LOPCM frequencies depend strongly on the free carrier density, allowing one to readily distinguish the coupled modes from the lattice modes whose frequencies are independent of the carrier density.

Excitation and detection of coherent oscillations were carried out with a degenerate pump–probe set-up described in detail elsewhere [4]. We used mode-locked Ti:sapphire laser pulses of 40 fs duration centred at 780 nm. The pulse train, with the repetition rate of 78 MHz, was divided into high intensity pump pulses and low intensity probe pulses. Both the pump and probe beams were kept close to normal incidence, being focused to a spot diameter of 50  $\mu\text{m}$ . The probe beam was polarized along the [110] direction of the sample, whereas the pump beam was along  $[\bar{1}10]$  direction. The power of the probe was 0.5 mW, and the ratio between the pump and probe powers was typically 100:1, unless specified otherwise. A time derivative technique with a shaker modulating the pump beam was employed to increase the signal-to-noise ratio of the coherent oscillations.

Representative time-domain results obtained at room temperature for differently doped InP films are shown in figure 1. It is apparent that the change of carrier concentration modifies the transient reflectivity on a femtosecond scale. The type of carrier also affects the signal: the oscillations are more pronounced and longer lived for p-type InP. This means that the polarizability of the lattice can be high enough to cause appreciable screening of the forces

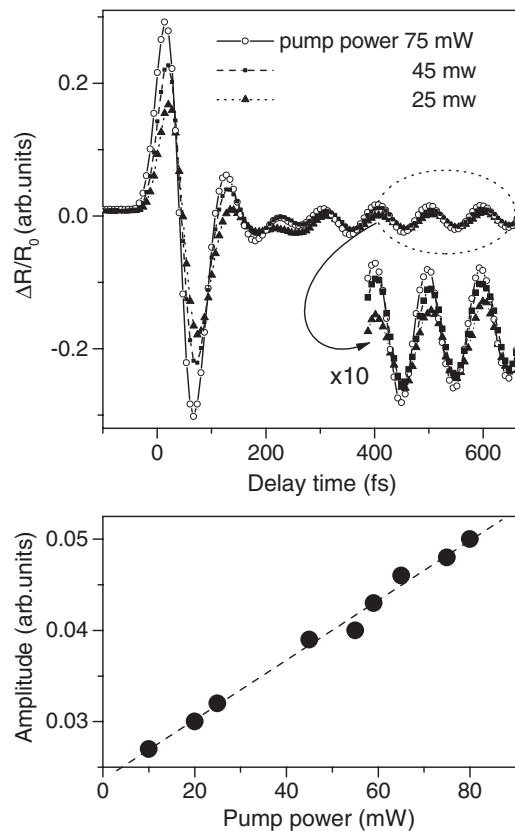


**Figure 2.** The upper panel illustrates the pump dependence for p-doped sample ( $N = 10^{18} \text{ cm}^{-3}$ ). The lower panel shows the coherent amplitude as a function of pump power (closed circles) together with the linear fit (dashed line).

between fluctuations in the charge densities of carriers, and thus, depending most probably on the initial phases of the density and lattice oscillations, one can observe either screening or antiscreening. There is no apparent change in the oscillation pattern at long delay times between p- and n-doped samples, which is in a striking contrast to the change of initial phase for the coherent oscillations reported for p- and n-type GaAs [5].

The major change introduced by doping is the alteration of the coherent amplitude and the modification of the frequency as well as the dephasing time. Also seen in figure 1 is that the decay of the coherence does not follow a single-exponential dependence; the coherent oscillations decay fast during the few first cycles and then the decay slows down. There are a number of possible explanations for the deviation from single-exponential decay. First, such a decay can mean that the relaxation time approximation, the one most frequently used to describe the coherent oscillations, is not applicable and the assumption of a constant decay rate is not adequate to our case. In this case, the non-exponential decay is a sign of either non-Markovian (the decay rate depends on history) or some other (let us say, the decay rate depends on time) behaviour. Second, the non-exponential decay can also arise from several frequencies being present in the complex oscillation with the decay times for the different modes being substantially distinct. However, if different modes with *comparable* decay times and amplitude are present one expects to see a beating pattern, which was not observed in our

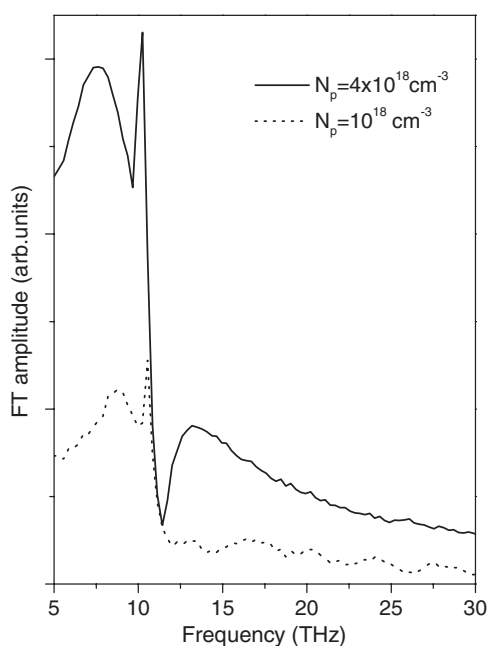


**Figure 3.** p-doped InP with  $N = 10^{18} \text{ cm}^{-3}$ . Fourier transforms (normalized at the LO frequency) of the pump-probe data for p-doped InP.

experiment. Since the approximations for non-Markovian and other behaviours have not been developed for coherent phonons and LOPCM, we will use the terminology of the relaxation time approximation for further discussion.

We observed that for a given carrier concentration, the oscillation decay and frequency do not appreciably depend on the pump power, whereas the oscillation amplitude varies with the pump power linearly, as illustrated in figure 2 for one of the p-doped samples. To measure the pump power dependence we kept the probe power constant and varied the pump power. The photoexcited carrier density  $N_{\text{exc}}$  estimated from the pump beam power density and the absorption coefficient varied from  $11 \times 10^{16}$  to  $9 \times 10^{17} \text{ cm}^{-3}$  in these experiments. The oscillation amplitudes shown in figure 2 were estimated for the third cycle. Note that for any sample at any pump power, the amplitude of oscillation at longer delay times never exceeds a few per cent of the overall reflectivity change just after the ultrafast excitation. This overall reflectivity change (measured with chopped light) is not seen in our data obtained with a shaker.

Fourier transformation of the oscillations revealed that the spectral content of the signal was modified with varying carrier concentration; see figure 3. The density dependent spectra shown in figure 3 for p-doped samples testify that the coupled modes are detected, since the lattice modes are independent of the electron/hole density. Additional information about the coupled phonon-plasmon dynamics can be obtained by analysing the time dependence of the Fourier transformed signal. To this end, we varied the lower bound of the sampled time interval, and the results obtained for the p- and n-doped samples are shown in figures 4 and 5, respectively. The detailed investigation for other carrier densities including the comparison to a frequency-domain study (Raman scattering) will be published in a forthcoming paper. In figure 4 the Fourier transformed data for the p-doped sample are normalized to unity at the LO phonon frequency and offset along the y-axis, whereas those in figure 5 for the n-doped sample are normalized at 8.8 THz, corresponding to most pronounced peak in the spectrum. These

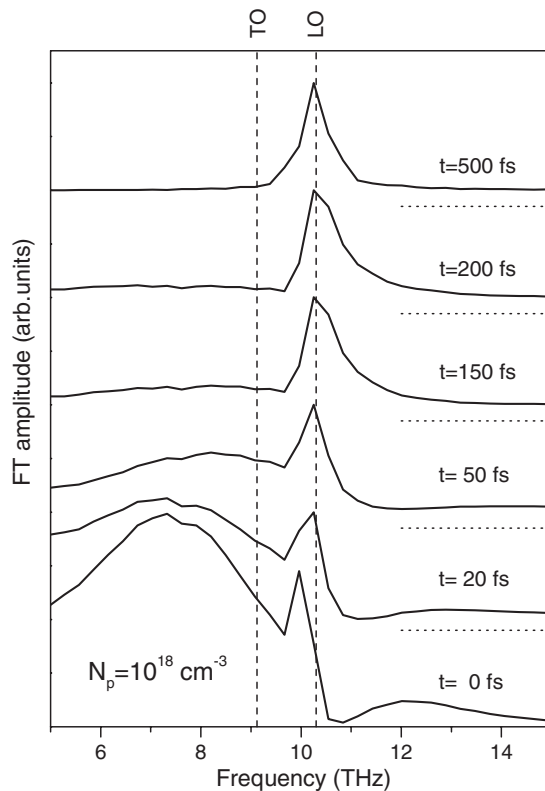


**Figure 4.** p-doped InP with  $N = 10^{18} \text{ cm}^{-3}$ . Fourier transforms (normalized at the LO frequency) of the pump–probe data with varying lower bound, indicated for each trace. The transforms are uniformly offset along the y-axis and the dashed lines running across the graph show the frequencies of LO and TO phonons. The baselines of each of the spectra are shown as dotted lined.

experiments complement frequency-domain Raman spectroscopy and allow one to extract information on fast dynamics. In contrast to the frequency-domain data case in which the short time dynamics must be extracted from the wings of a spectral line where the signal-to-noise ratio is poorest, in the time domain the fast dynamics are observed with the highest signal-to-noise ratio (the signal is maximal at short time delays). As seen from the last two figures, the spectral content changes with time, and immediately after the excitation the spectrum clearly shows the existence of LOPCM. Since the decay for the LOPCM is fast, after a few hundreds of femtoseconds it disappears from the spectrum of the p-doped sample. However, the peak at the unscreened LO frequency remains asymmetric in lineshape, relaxing to a Lorentzian form after only 500 fs. The dephasing time for uncoupled LO phonons considerably exceeds that for coupled plasmon–phonons and, as a result, the short time dynamics is dominated by the coupled LO–plasmon modes, whereas for longer time delays the coherent dynamics is governed by the lattice mode alone. The long time dynamics of the two p-doped samples were essentially similar and dominated by unscreened LO phonons. However, for n-doped samples the lower branch of the LOPCM decays more slowly than in the case of p-doped samples. As seen from figure 4, the long time dynamics were determined by the lower branch of the LOPCM (note that the frequency does not coincide with that of the TO phonon). From the fits, we determined the spectrum parameters for one particular ( $N_p = 10^{18} \text{ cm}^{-3}$ ) concentration: bare LO phonon:

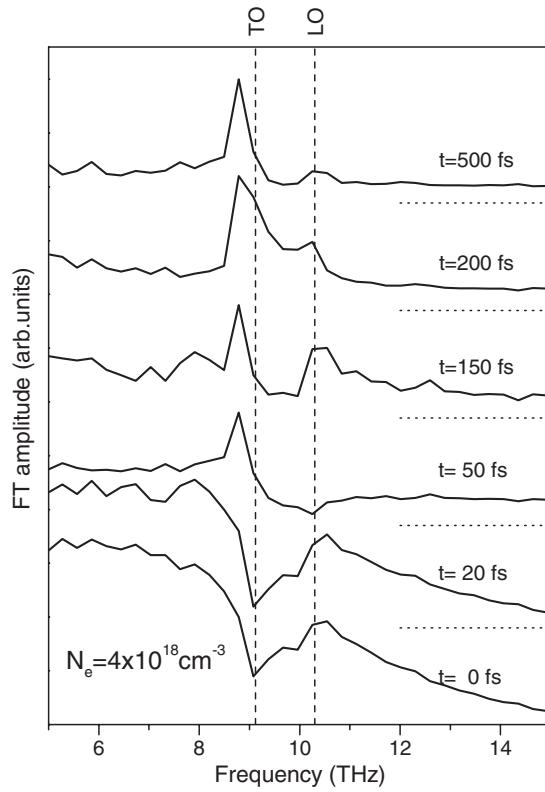


**Figure 5.** The same as figure 3, but for n-doped InP with  $N = 4 \times 10^{18} \text{ cm}^{-3}$ , and the normalization made at 8.8 THz. The baselines of each of the spectra are shown as dotted lined.

$\bar{\nu} = 10.3 \text{ THz}$  and  $\Delta\nu = 0.5 \text{ THz}$ ;  $\text{LO}_+$ :  $\bar{\nu} = 12.3 \text{ THz}$  and  $\Delta\nu = 2.2 \text{ THz}$ ; and  $\text{LO}_-$ :  $\bar{\nu} = 7.2 \text{ THz}$  and  $\Delta\nu = 4.8 \text{ THz}$ . In addition, even for the lowest carrier concentrations, we did not observe any spectral dependence on the pump power for any type of doping. However, as mentioned before, the spectra obtained with the lower bound for the Fourier transform fixed at zero were different for differently doped samples. In this respect, InP behaves distinctly differently from GaAs for which the coupled mode frequencies were reported to be pump power dependent [5]. In our experiments on InP, the most pronounced dependence for the coupled mode frequencies (at least for the low fluence regime, with fluence in the  $\mu\text{J cm}^{-2}$  range) was observed for the background carrier density, since the photoexcited density never exceeds the background carrier density.

Although the time- and frequency-domain techniques actually measure two *different* systems—the coherent, with a well-defined phase relationship, and the thermal, where the phase is random, we will cite typical values obtained for InP by means of Raman scattering at room temperature: LO frequency and linewidth —10.3 and 0.037 THz, respectively, TO frequency —9.12 THz [10, 11]. Note that while the frequencies of the LO phonon are the same, within the experimental error, for the pump–probe and Raman data, the phonon damping rate measured by the Raman method is significantly smaller than the dephasing rate probed in the time domain.

For comparison purposes, we carried out similar pump–probe experiments on low temperature grown n-GaAs with the background electron density of  $9 \times 10^{17} \text{ cm}^{-3}$ . The time-

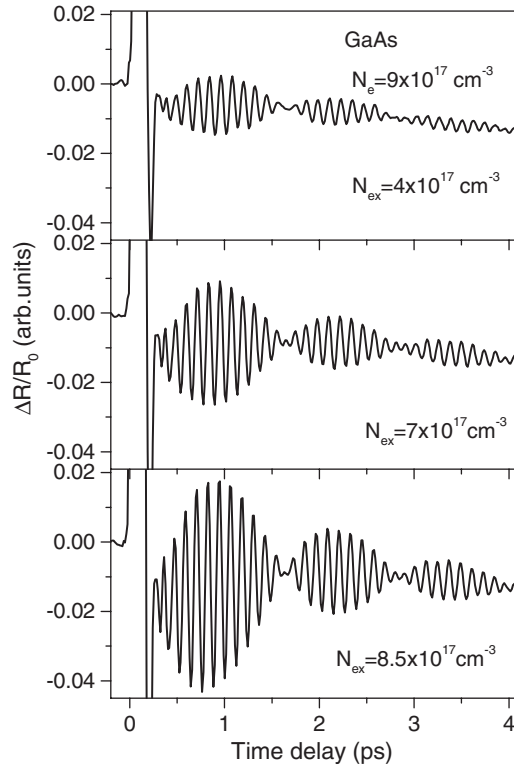


**Figure 6.** Differential reflectivity as a function of time delay for n-doped GaAs with the free carrier concentration of  $N = 9 \times 10^{17} \text{ cm}^{-3}$  for different excitation levels, shown in each panel.

domain data for GaAs exhibit a pronounced beating pattern originating from the coupling of a coherent LO phonon and a plasmon contribution centred around the TO phonon frequency (the screened LO mode); see figure 6. Changing the photoexcited carrier density  $N_{\text{exc}}$  we observed increased visibility of the interference pattern, whereas the spectral content remained essentially unchanged; see figure 7. This is primarily due to the fact that the spectrum is defined by the total carrier density given by the sum of the background electron density and the excited electron density in which the background density dominates. Detailed spatially resolved studies on GaAs [3, 5] made it clear that the pronounced beating pattern originated from different contributions within the laterally inhomogeneous plasma. It should be noted that our results on GaAs are almost identical to those obtained in [6] except as regards the absence of the upper branch of the coupled phonon–plasmon mode, which is due to a longer pulse duration being used in our experiments. Given that the band structures, and thus the Fröhlich constants and the deformation potentials, of gallium arsenic and indium phosphate are similar, it is difficult to conceive of a reason for which the non-equilibrium coupled modes in the two crystals should be different. We consider that the effects of lateral carrier inhomogeneities (especially when using same pump and probe spot sizes) as well as the carrier distribution of the doping carriers as a result of electric field screening [12] are responsible for the different behaviours of non-equilibrium coupled modes. These effects can strongly suppress the observation of well-defined coupled plasmon–phonon modes or well-defined beating patterns [3]. Like that of the lateral inhomogeneity caused by equal spot sizes of the pump and probe, we cannot



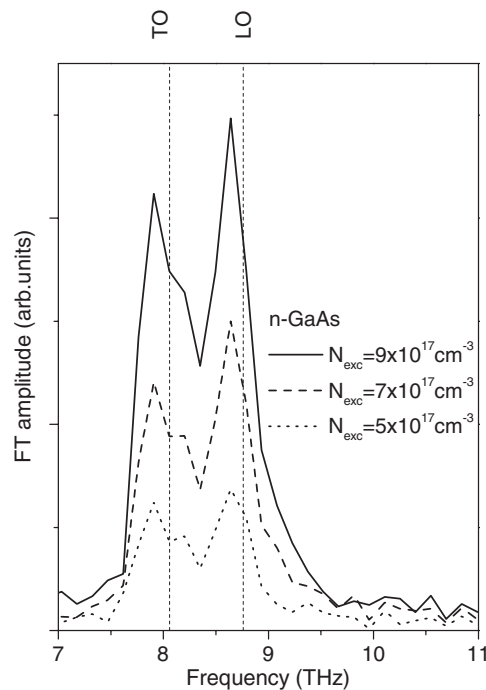


**Figure 7.** Fourier transforms of the pump-probe data for n-doped GaAs at different excitation levels. The dashed lines running across the graph show the frequencies of LO and TO phonons.

exclude the contribution of the through-depth inhomogeneity. Indeed, it is well known that the photoluminescence efficiency of GaAs is much less than that of InP [13]. This is usually considered indicative of the much larger surface recombination velocity in GaAs, leading to the extremely inhomogeneous carrier density generated by the pump pulses perpendicular to the surface.

To summarize the experimental results, the important features of the data, which can be informative, are

- (i) the spectra obtained through the Fourier transformation of the femtosecond reflectivity are density dependent;
- (ii) the spectra of p-doped samples are time dependent and clearly show the LOPCM at short delay times, whereas the spectrum at longer delay times is exclusively determined by lattice modes;
- (iii) the spectra of n-doped samples demonstrate that the plasmon dephasing time can be increased by the coupling to the lattice.

This clearly shows that the coupling with the coherent lattice motion can effectively prolong the coherence of collective electron motion.

To fully understand the temporal behaviour following the ultrafast excitation of indium phosphate, a number of points should be clarified. Among the most important are the following: the mechanisms of generation and detection of photoinduced coherence; the influence of possibly inhomogeneous conditions for the photogenerated plasma; and the band structure effects. Without going into detail on any of these, we just mention that any macroscopic variable that interacts with the electron and/or lattice can be used to drive the coherent oscillations

provided that it can be switched on a timescale shorter than the oscillation's period. For GaAs with the same zinc-blende structure as InP, the driving force of the coherent oscillations was ascribed as the electric field in the depletion layer. According to the analysis by Cho *et al.*, the electric field in the depleted layer is the main cause of both the coherent phonon and coupled phonon–plasmon modes in GaAs [5]. This has also been proved in a theoretical study [14]. Given the same zinc-blende crystal structure as A<sup>III</sup>B<sup>V</sup> semiconductors, which is responsible for the symmetry selection rules, a similar mechanism may act in InP. Alternatively, the driving mechanism could be reduced to light stimulated excitation of coherent oscillations in a dispersive limit [2]. Note though that the first-order Raman tensor of InP is off-diagonal; the LO phonon and/or LOPCM can usually be observed in the polarized spectrum through the impurity induced Fröhlich interaction. At resonance, the dipole-forbidden scattering (observed in a polarized spectrum) can be comparable to the dipole-allowed scattering (observed in a depolarized spectrum), and with our experimental geometry we probe fully symmetric excitations that are accessible in Raman scattering for the  $x'x'$  and  $y'y'$  polarizations. We verified the isotropic nature of the observed signal by measuring the responses for the pump polarization along [110] and [010] directions.

In conclusion, we have experimentally studied femtosecond time-resolved optical responses of differently doped p- and n-type InP. It has been proved that LOPCM of InP can be observed in the time-domain study. This conclusion was reached from the density dependence of the observed oscillation frequency revealed through temporal analysis of the spectra. Comparison to the data available for GaAs has revealed a notable difference between the two systems, most probably caused by lateral and depth carrier inhomogeneities. We have observed that the coupled mode frequencies in InP depend strongly on the background carrier density and are, in the low fluence regime, almost independent of the photoinduced density.

## Acknowledgment

The authors appreciated support from the Russian Foundation for Basic Research through grant No 04-02-97204.

## References

- [1] Shah J 1996 *Ultrafast Spectroscopy of Semiconductors and Semiconductors Nanostructures* (Berlin: Springer)
- [2] Merlin R 1997 *Solid State Commun.* **102** 207
- [3] Dekorsy T, Cho G C and Kurz H 2000 *Light Scattering in Solids VIII* ed M Cardona and G Günterodt (Berlin: Springer) p 169
- [4] Misochko O V 2001 *Zh. Eksp. Teor. Fiz.* **119** 246  
Misochko O V 2001 *JETP* **92** 285 (Engl. Transl.)
- [5] Cho G C, Dekorsy T, Bakker H J, Hovel R and Kurz H 1996 *Phys. Rev. Lett.* **77** 4062  
Cho G C 1998 *Proc. SPIE* **3277** 44
- [6] Hase M, Nakashima S, Mizoguchi K, Harima H and Sakai K 1999 *Phys. Rev. B* **60** 16526
- [7] Granin E D, Tsen K T and Ferry D K 1996 *Phys. Rev. B* **53** 9847
- [8] Nakashima S, Mizoguchi K, Harima H and Sakai K 1998 *J. Lumin.* **76/77** 6
- [9] Leitenstorfer A, Hunsche S, Shah J, Nuss M C and Knox W H 2000 *Phys. Rev. B* **61** 16642
- [10] Olego D and Cardona M 1981 *Phys. Rev. B* **24** 7217
- [11] Kauschke W and Cardona M 1986 *Phys. Rev. B* **33** 5473
- [12] Dekorsy T, Pfeifer T, Kutt W and Kurz H 1993 *Phys. Rev. B* **47** 3842
- [13] Casey H C Jr and Buchler E 1977 *Appl. Phys. Lett.* **3** 247
- [14] Cusco R, Ibanez J and Artus L 1998 *Phys. Rev. B* **57** 12197